Biophysical *Journal*
Article

Biophysical Society

β Cells Operate Collectively to Help Maintain Glucose Homeostasis

Boris Podobnik,[1,2,4,5,6,*] Dean Korošak,[7,8] Maša Skelin Klemen,[7] Andraž Stožer,[7] Jurij Dolenšek,[7] Marjan Slak Rupnik,[7,9,10,*] Plamen Ch. Ivanov,[3,11,12] Petter Holme,[13] and Marko Jusup[13]

[1]Faculty of Civil Engineering, University of Rijeka, Rijeka, Croatia; [2]Center for Polymer Studies and [3]Keck Laboratory for Network Physiology, Department of Physics, Boston University, Boston, Massachusetts; [4]Zagreb School of Economics and Management, Zagreb, Croatia; [5]Luxembourg School of Business, Luxembourg, Luxembourg; [6]Faculty of Information Studies in Novo Mesto, Novo Mesto, Slovenia; [7]Institute of Physiology, Faculty of Medicine and [8]Faculty of Civil Engineering, Transportation Engineering and Architecture, University of Maribor, Maribor, Slovenia; [9]Center for Physiology and Pharmacology, Medical University of Vienna, Vienna, Austria; [10]Alma Mater Europaea-European Center Maribor, Maribor, Slovenia; [11]Harvard Medical School and Division of Sleep Medicine, Brigham and Women's Hospital, Boston, Massachusets; [12]Institute of Solid State Physics, Bulgarian Academy of Sciences, Sofia, Bulgaria; and [13]Tokyo Tech World Research Hub Initiative (WRHI), Institute of Innovative Research, Tokyo Institute of Technology, Tokyo, Japan

ABSTRACT Residing in the islets of Langerhans in the pancreas, β cells contribute to glucose homeostasis by managing the body's insulin supply. Although it has been acknowledged that healthy β cells engage in heavy cell-to-cell communication to perform their homeostatic function, the exact role and effects of such communication remain partly understood. We offer a novel, to our knowledge, perspective on the subject in the form of 1) a dynamical network model that faithfully mimics fast calcium oscillations in response to above-threshold glucose stimulation and 2) empirical data analysis that reveals a qualitative shift in the cross-correlation structure of measured signals below and above the threshold glucose concentration. Combined together, these results point to a glucose-induced transition in β-cell activity thanks to increasing coordination through gap-junctional signaling and paracrine interactions. Our data and the model further suggest how the conservation of entire cell-cell conductance, observed in coupled but not uncoupled β cells, emerges as a collective phenomenon. An overall implication is that improving the ability to monitor β-cell signaling should offer means to better understand the pathogenesis of diabetes mellitus.

SIGNIFICANCE Distributed into about a thousand to a million separate micro-organs called islets, pancreatic β cells keep a delicate metabolic balance known as glucose homeostasis via heavy cell-to-cell communication within the physical limits of an islet. Such communication implies that both nutrient sensing and controlled insulin release emerge as collective processes instead of being encoded directly into individual β cells. We used dynamical networks to obtain simulated cell activity that faithfully mimics empirical signals and to show that network nodes, as the theoretical equivalent of cells, preserve their statistical properties during normal operation. From a mechanistic standpoint, the results corroborate that living cell systems, just like modeled dynamical networks, ensure sensitivity to threshold glucose stimulation through coordinated action.

INTRODUCTION

On a fundamental level, living tissues comprise genetically identical cells of the same differentiation fate that work cooperatively to support homeostasis and other physiological functions (1). Cooperation, however, is susceptible to cheating unless there is a mechanism for mutual recognition of cooperators referred to as positive assortment (1). Cell-to-cell communication is perhaps the most obvious means of positive assortment, employed even by cancer cells—quintessential cheaters from the perspective of normal tissue functioning—to successfully metastasize (2). A key question in this context is how, in large clusters of cells (e.g., tissues or organs), cluster-wide functionalities emerge as collective phenomena from local cellular interactions (e.g., communication and cooperation) encoded into individual cells. Endocrine cells in pancreatic islets, in particular, form well-defined cellulosocial clusters, each ∼100 μm in size. Intriguingly, islet size is persistent across multiple vertebrate species (3,4), thus fueling conjectures that

Submitted December 6, 2019, and accepted for publication April 6, 2020.

*Correspondence: bp@phy.hr or marjan.slakrupnik@meduniwien.ac.at

Editor: James Keener.

https://doi.org/10.1016/j.bpj.2020.04.005

cross-species size persistence plays a vital role in the collective functioning of a healthy islet (5,6).

β cells are a type of pancreatic cell that participate in glucose homeostasis by producing, storing, and releasing the hormone insulin (7–9). When the glucose blood level is high, a state known as hyperglycemia, β cells respond with a release of insulin into the bloodstream to promote nutrient import and storage in a variety of cells in support of anabolic metabolism (10). When the glucose blood level is low, a state known as hypoglycemia, or glucose is otherwise in demand, e.g., because of physical activity, β cells switch off insulin secretion to allow catabolic metabolism. β cells thus employ a negative feedback mechanism to help maintain the blood glucose within a safe range. In comparison, therapeutic administration of insulin in diabetic patients lacks the precision of the internal regulatory processes, yielding either too high or too low plasma glucose levels (11). Hypoglycemic episodes arising in relation to insulin therapy are a common adverse effect of antidiabetic therapies (12). Although the basic outline of glucose homeostasis is conceptually clear, complexity quickly escalates when looking for a microscopic understanding of the negative feedback mechanism employed by β cells. We herein attempt to better understand this complexity, focusing in particular on cell-to-cell communication in the face of mounting evidence that such communication is important for insulin secretion and, by extension, glucose homeostasis (8,9,11).

Illustrating microscopic complexity, cellular nutrient-sensing mechanisms (13,14) have been shown to intermix metabolic signals, electrical activity, and cytosolic calcium signaling (15–18). This complex intermix prevents β cells of a healthy pancreas from oversecreting insulin despite huge intracellular insulin stores (19), which exceed the lethal dose by two to three orders of magnitude if released at once. A possible answer to how β cells regulate their secretion may lie in a response of β-cell collectives to above-threshold glucose concentrations (>7 mM in mice (20,21)), at which electrical and calcium activities flip between nonstimulatory and stimulatory phases. Here, the term collective is used to denote the fact that β cells, in addition to engaging in paracrine interactions (22,23), are coupled to neighboring β cells via gap junctions (comprising two connexons of Cx36 protein) to form a communicating functional syncytium (24). This functional syncytium as a whole reacts to nutrients (e.g., glucose) or pharmacological substances (e.g., sulphonylureas) in a fundamentally different manner from isolated cells (25) or partially "uncoupled" cells, i.e., those lacking the Cx36 protein (26–28). Specifically, after closing ATP-sensitive K^+ channels in a coupled configuration, the remaining entire cell-cell conductance varies among individual cells but stays constant and relatively high islet wide. This happens throughout the timeframe of a typical experiment (>10 min) and despite the concurrent dynamic interchange of nonstimulatory and stimulatory collective phases (26).

A series of models describing fast Ca^{2+} oscillations in the electrical activity of β cells have been constructed since the first minimal model over three decades ago (29). The primary purpose of these models, however, has been to generate the saw-tooth time profile characteristic of slow processes underlying the observed electrical bursting (30,31). By contrast, there seem to have been much less concern with the oscillatory response of β cells to the threshold glucose concentration, and the relationship of this response to communication within the functional syncytium or the conservation of entire cell-cell conductance (32).

We demonstrate that a cell-to-cell communication model based on a dynamical network approach (33,34) captures the essential features of fast Ca^{2+} signaling and that within such a model, the simulated equivalent of the entire cell-cell conductance remains conserved in a statistical sense after the network transitions from an inactive to an active state, thus suggesting that the same mechanism may be at work in a living cell system as well. To provide empirical support for these results, we proceed with probing correlations in fast Ca^{2+} signaling as a measure of cell-to-cell communication, and present evidence of a shift in the correlation structure between nonstimulatory and stimulatory conditions. This shift is consistent with expectations from the modeled dynamical network and the idea that sensitivity to glucose stimulation via collective action differs substantially from the sensitivity of individual cells. Note that we are not trying to contrast our model and its outputs to the existing models of coupled deterministic oscillators derived from the prevailing Hodgkin-Huxley paradigm. In fact, there is no conflict between the two approaches, at least not conceptually. We simply show that in a collection of cells, no special deterministic mechanism is needed to generate collective responses that come remarkably close to the empirically observed patterns.

METHODS

We analyzed a data set obtained by Ca^{2+} imaging of acute pancreatic tissue slice (35,36) comprising rodent pancreatic oval-shaped islet (approximate dimensions: 370 × 200 m). We recorded Ca^{2+} signals with a functional multicellular imaging technique at 10 Hz and 256 × 256 pixel resolution in eight-bit grayscale color depth. The data set consisted of 65,536 traces of calcium signals, each 23,873 time steps long. During the recording, we increased glucose concentration in the chamber containing the tissue sample from 6 to 8 mM and then decreased it back to the initial concentration near the end of the experiment. We chose these two physiological glucose concentrations to induce a transition from a nonstimulatory to a stimulatory β-cell phase. The typical threshold for this transition in mice is around 7 mM (20,21). Further methodological details, including an ethics statement, are available in the Supporting Materials and Methods.

Individual Ca^{2+} traces, as well as the ensemble-averaged signal, exhibit 1) slow calcium oscillations with a period of ~5 min but also superimposed 2) fast calcium oscillations (Fig. 1 *A*). We detrended all traces as a part of signal preprocessing to exclude the effect of systematic slow diminishing of

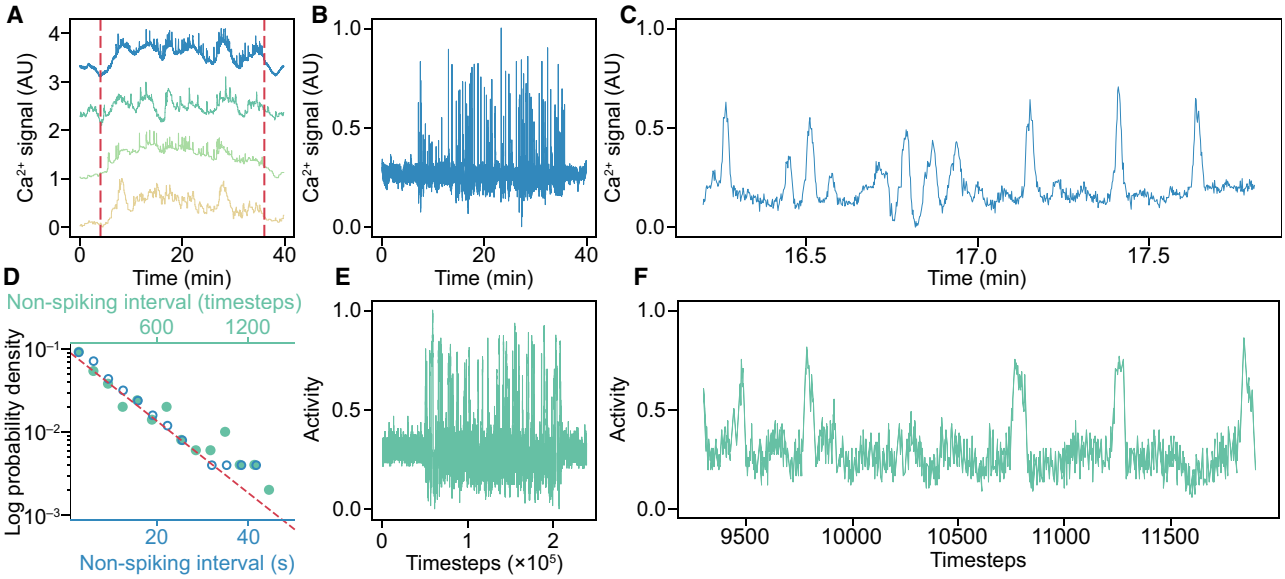

FIGURE 1 β-cell Ca^{2+} signaling is faithfully mimicked by a cell-to-cell communication model. (*A*) Examples of the detrended experimental traces of Ca^{2+} signaling, including the ensemble average (*top trace*), are shown. Vertical red lines denote the time interval during which we perfused the tissue slice with 8 mM glucose solution. Otherwise, we kept the tissue slice in 6 mM glucose solution, which is below the typical threshold for glucose-stimulated activity of β cells. (*B*) The ensemble average of the measured fast Ca^{2+} signaling is shown. The transitions from a nonstimulatory glucose to a stimulatory glucose phase and vice versa are clearly visible. (*C*) A detail of the ensemble average of the measured fast Ca^{2+} signaling in the stimulatory phase is shown. Spikes of exceptionally high activity are interspersed among somewhat quieter periods. (*D*) The probability distribution of time interval Δt between two consecutive $+1$ states in the binarized signal (Fig. S2 *C*) is shown. Open dots represent the empirical distribution for the ensemble-averaged fast Ca^{2+} signaling component in a semilog plot. The dashed line is a theoretical distribution function, $\rho\exp(-\rho t)$, with mean rate $\rho = 10$ s. Among our primary goals was to reproduce the described empirical patterns using a cell-to-cell communication model (details in the main text). Solid dots thus represent the distribution of interval Δt for the simulated fast β-cell activity. (*E*) Our cell-cell communication model with $N = 100$ cells successfully mimics fast Ca^{2+} signaling (cf. *B*). While transitioning from a nonstimulatory (6 mM) to a stimulatory (8 mM) glucose solution in the experiment, we set the model's forcing parameter, i.e., cell responsivity, to a higher value. (*F*) A detail of the simulated fast β-cell activity is shown. Despite a somewhat higher baseline noise compared to measurements in this particular example (cf. *C*), the two signals are statistically equivalent (see also Fig. S3). To see this figure in color, go online.

the signal with time (Fig. S1). Calcium oscillations on both timescales are known to be accompanied with insulin release (37,38), but the saturation kinetics of the Ca^{2+}-dependent insulin release suggests that faster oscillations dominate (39). The relation between slow calcium oscillations and pulsating insulin release was comprehensively described in a recent review (31). Here, by contrast, we focus on fast calcium oscillations, which in acute pancreatic slice preparations, like in early microelectrode recordings (40), directly correspond to membrane electrical bursting activity (21,41) and are thought to be functionally relevant for glucose homeostasis (42).

To isolate fast calcium oscillations, we proceeded by removing slow oscillations from traces using a total-variation-based filter (https://github.com/albarji/proxTV) (Fig. S2; (43)). The structure of the remaining fast calcium signal (Fig. 1 *B*) clearly separates the nonstimulatory phase with little calcium activity from the stimulatory phase with large oscillation amplitudes. In both phases, the signal is stochastic in nature (Fig. 1 *C*), which can be analyzed using statistical measures. We thus binarized the fast component of the ensemble-averaged Ca^{2+} trace to distinguish between large calcium spikes (marked $+1$) or the lack thereof (marked -1). We subsequently estimated the distribution of time interval Δt between two consecutive $+1$ states in the binarized trace (Fig. S2 *C*). We found that interval Δt is governed by a Poisson process, implying that the corresponding probability density function (pdf) can be approximated with exponential distribution $\rho\exp(-\rho t)$, where the mean rate equals $\rho = 10$ s (*open dots* in Fig. 1 *D*). Interestingly, a dynamical network model of cell-to-cell communication produces a simulated fast signal with the same statistical characteristics (*solid dots* in Fig. 1 *D*). We next describe this model and some of its basic properties.

RESULTS

Emerging properties of β-cell-to-β-cell communication

Glucose homeostasis is a complex phenomenon involving multiple cell types and hormones. Our stylized approach, however, focuses on β cells alone and, in particular, the role of cell-to-cell communication in shaping the response of these cells to the threshold glucose concentration. Specifically, we constructed a dynamical network model in which N network nodes represent individual β cells and network links represent couplings with k neighboring cells (Fig. 2). A node, in contrast to commonly assumed coupled oscillators (44), is stripped of any structure beside being active or inactive. The model's key assumption is that nodes change their state internally or externally, with the former being modulated by the presence or absence of stimulatory glucose concentration, whereas the latter is due to cell-to-cell communication. An internal transition of a node from active to inactive state over time period dt occurs with probability pdt. Conversely, a transition prompted by mutual communication occurs with probability rdt, but only if the

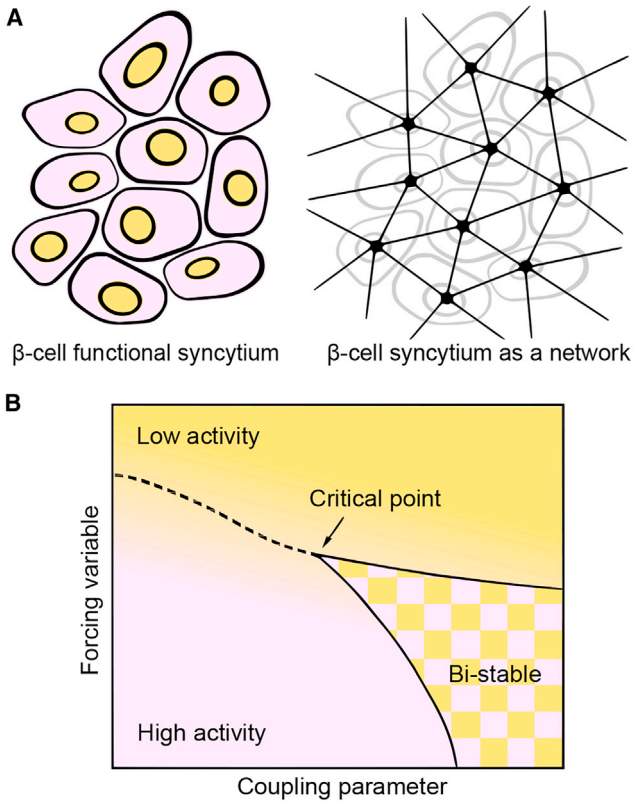

FIGURE 2 Model schematics. (*A*) We adapted a general dynamical network model (33) in such a way that N network nodes represent individual β cells and network links represent couplings with k neighboring cells. Each node can be in one of the two states, inactive or active, reflected in the amplitude of fast calcium signal. The state of the network in a particular time step is characterized by the fraction of active nodes. (*B*) Network activity is primarily modulated by a forcing variable, assumed inverse proportional to the glucose concentration, and a coupling parameter, assumed constant to a first approximation given the conserved cell-cell conductance (see Fig. 4 and related text). For small values of the coupling parameter, the system's collective property is weak, the distinction between inactive and active phases is blurred, and a response to forcing is quasilinear. Closer to the critical point, the collective property enables a steep, nonlinear response to forcing. Far beyond the critical point, the collective property would be overexpressed and the response to forcing muted. To see this figure in color, go online.

node has less than $m < k$ active neighbors. Nodes return to their original state after relaxation times τ_i and τ_e after an internal or an external transition, respectively. The state of the network is characterized by the fraction of active nodes.

Once node relaxation is defined, the network's state is determined by two parameters, probability rate r and the average fraction of internally inactive nodes, which follows from probability rate p via $p^* = 1 - \exp(-p\tau_i)$ (33). In two-parameter phase space, (r, p^*), there is a critical point that opens a bistability region separating low- and high-activity model equilibria (33,34). When network parameters approach the critical point, node activity suddenly picks up, whereas inside the bistability region, even spontaneous phase flipping becomes possible (33,34).

To illustrate similarities between model outputs and recorded Ca^{2+} traces (cf. Fig. 1, *B* and *C* and Fig. 1, *E* and *F*), we ran exhaustive numerical simulations (Remark 1 in the Supporting Materials and Methods). First, we created a random regular network with $N = 100$ nodes, each with $k = 10$ neighbors, in which the threshold for external inactivation was set to $m = 4$. We then chose $r = 0.78$, $\tau_i = 10$, and $\tau_e = 1$ as the parameter values that faithfully reproduce the characteristics of recorded Ca^{2+} traces (Fig. S3). Finally, we began simulations with $p^* = 0.90$ to place the network into the inactive part of the phase space but subsequently decreased this value to $p^* = 0.28$ to position the network close enough to the critical point for the activity to pick up substantially (Fig. S4; see also Fig. S5 for some additional model properties near the critical point). The decrease of p^* follows a decrease in probability rate p, which in turn is a response to an increased glucose concentration. As mentioned, the presence or absence of stimulatory glucose concentration modulates the response of individual β cells, whereas the response of the β-cell collective remains muted until a certain critical threshold of individual cell activity is reached. This behavior mimics the idea, first proposed by modeling studies (45) and then empirically validated (26), that the concentration response of an average electrical activity in β-cell collectives is steep with respect to glucose sensing. Cell-cell coupling thus narrows the glucose concentration range that induces or stops insulin secretion, which is in sharp contrast with Cx36-deficient mice, whose inability to synchronize β-cell activation, activity, and deactivation leads to increased basal insulin release (26,28,46).

As with the recorded fast calcium oscillations, we calculated the pdf of time interval Δt between two consecutive $+1$ states in the binarized network activity and found the same Poisson process as in the recorded data (cf. *open* and *solid dots* in Fig. 1 *D*). This calculation, in particular, shows that the similarities between measurements and simulations are not just superficial but extend into the statistical domain, as well.

To strengthen the case for similarity between measurements and simulations in the statistical domain, we compared additional statistics implied by the data and predicted by the model. To this end, we first differenced both measurements and simulations to generate more stationary time series of fluctuations. Differencing is a standard tool in time-series analysis that produces a new time series by taking differences between successive—possibly with a small time lag—terms in the original time series. We subsequently estimated the pdf of obtained fluctuations and looked for an underlying theoretical distribution that fits the results well (Fig. 3). We found a remarkable correspondence between the pdf estimated from the data and the one estimated from the model predictions. The underlying theoretical distribution is strongly non-Gaussian and consistent with a Lévy α-stable distribution with parameter

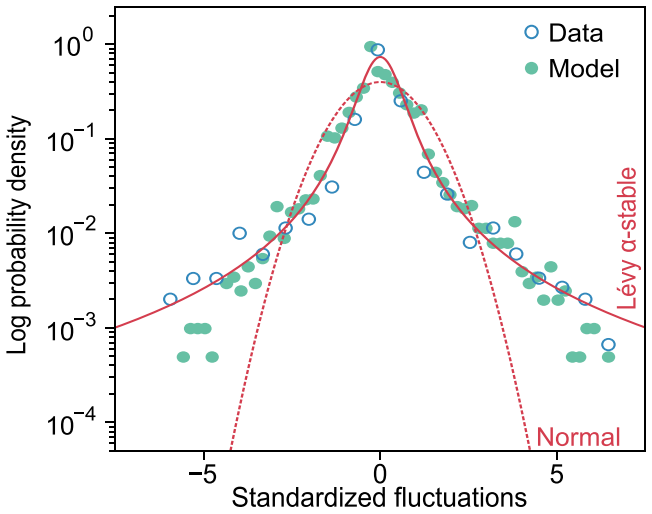

FIGURE 3 Cell-to-cell communication model predicts statistical properties of measured signals. Denoting the original time series by $X(t)$, the estimated probability density functions (pdfs) of fluctuations $Z(t) = X(t) - X(t - \Delta t)$ are shown, where $\Delta t = 10$ time steps is delay time. Similarity between the pdfs estimated from empirical calcium signals and network model activity is remarkable. Furthermore, the two pdfs are strongly non-Gaussian, which, in complex systems such as the studied functional β-cell syncytium, signifies important nonlinearities and couplings. The solid curve is a Lévy α-stable distribution with parameter $\alpha = 1.3$, whereas the dashed curve is a Gaussian distribution with a zero mean and a unit variance. To see this figure in color, go online.

$\alpha \approx 1.3$ (Fig. 3). The Lévy α-stable distribution is a signature of nonlinearities and couplings in complex systems that arise when a system's components coordinate action and function in unison (47). We thus see that our model is capable of predicting the statistical properties of measured signals and that these predictions theoretically underpin the collective operation of β cells.

A link between any node pair in the dynamical network corresponds to coupling between β cells. This coupling enables cell-to-cell communication and collective sensing (5), during which a β cell communicates with its neighboring β cells through gap junctions and, within a limited range, using paracrine signals (5). A basic description of the need for communication among heterogeneous β cells in an islet has been around for some time (48) but has only recently been revived in the light of efficient high-throughput analyses. Such analyses enabled the identification of a number of functional and nonfunctional cell subpopulations with their characteristic genetic and expression profiles, incidences, and diabetes-related changes (14,49–51).

Here, we could naturally model the heterogeneity of β-cell communication channels with the strength of links between neighboring cells. Following the ideas proposed for interneuronal dynamics and synaptic strength (34), in each time step, we strengthened the link between two active nodes in the network by ε with probability p_s and weakened by $z\varepsilon$ with probability $1 - p_s$. If either of the nodes is inactive, we weakened link strength by $z\varepsilon$. Surprisingly, this simple local rule leads to the emergence of a statistical conservation law for the strength of network links as a collective phenomenon (34). We demonstrated this using the same set of parameters as in Fig. 1 *E* and setting $\varepsilon = 0.001$ and $z = 0.07$. We additionally set the initial values of link strengths by drawing randomly from an exponential distribution with unit mean and sufficient standard deviation to capture the heterogeneity of entire cell-cell conductances between pairs of β cells (52). When the network is highly active (Fig. 4 *A*), link strengths increase or decrease depending on the activity of individual nodes, creating a wide range of possible outcomes (Fig. 4 *B*). The ensemble average link strength, however, is conserved, thus showing that the collective exhibits a property, namely the statistical conservation of link strength, that is not embedded into any individual node. This modeled property corresponds to the islet-wide

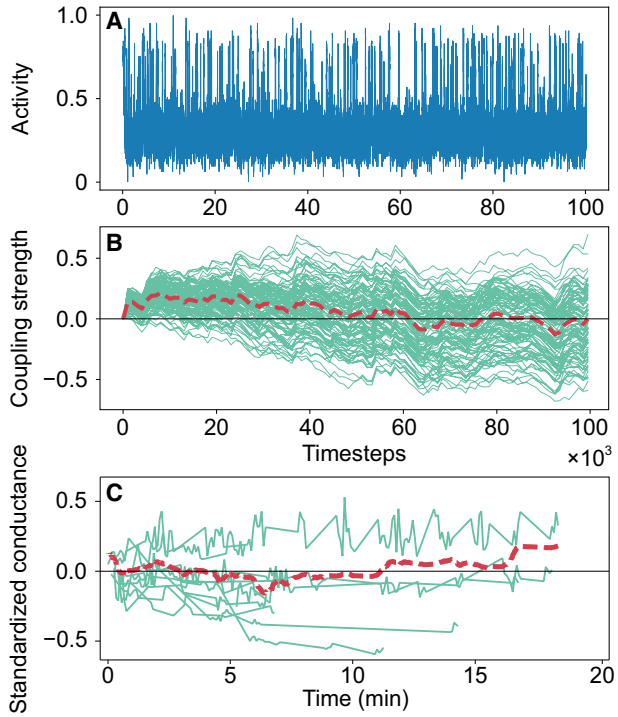

FIGURE 4 Conserved entire cell-cell conductance of coupled β-cells in stimulatory glucose phase is an emergent collective property. (*A*) Shown is the simulated dynamical network activity in the stimulatory phase using the same parameters as in Fig. 1 *E*. In simulations, β cells are represented by nodes and cell coupling by links. Each link has a different coupling strength that varies depending on the dynamical network's activity. (*B*) The conservation of coupling strength emerges collectively. Coupling between any pair of linked nodes can either decrease or increase in strength (*green solid paths*), but the ensemble average (*red dashed path*) remains unchanged within the limits of statistical fluctuations. (*C*) Empirical data qualitatively confirm the model results. For the purpose of measuring the time-varying residual conductance, the individual mouse β cell in an intact islet in a pancreatic slice has been dialyzed with 5 mM ATP solution to block the K_{ATP} channels ($n = 10$). The red dashed path represents the running average of all shown measurements. To see this figure in color, go online.

conservation of the entire cell-cell conductance seen in experiments (Fig. 4 *C*; (26)).

Empirical evidence of β-cell collective behavior

If the response of cells to glucose is indeed a collective phenomenon, this should be visible in cell-to-cell communication patterns below and above the threshold glucose concentration. Taking into account that the intensity of cell-to-cell communication is mirrored by the cross-correlation structure of measured signals (Remark 2 in the Supporting Materials and Methods; see also Fig. S6), we explored this structure by randomly selecting 4000 Ca^{2+} traces and calculating cross correlations

$$C_{ij} = \frac{\langle s_i s_j \rangle - \langle s_i \rangle \langle s_j \rangle}{\sigma_i \sigma_j} \tag{1}$$

between two traces s_i and s_j at positions $i = (x_i, y_i)$ and $j = (x_j, y_j)$, where σ_i and σ_j are the standard deviations of the traces. To cancel noise, we turned individual cross correlations into a function of distance $C(d) = \langle C_{i,j} \rangle$, where $\langle \bullet \rangle$ indicates averaging over all distances $d_{ij} \in [d - d_0, d + d_0]$ with $d_0 = 5$ pixels. We calculated $C(d)$ separately for the nonstimulatory and stimulatory phases, focusing especially on the differences between them.

In the limit of short distances, which are typical distances between the pixels inside a single β cell, the cross correlations in both phases are similar. Important quantitative differences emerge at pixel distances above 10. Interpreting function $C(d)$ as a power-law decay with a faster-than-exponential cutoff

$$C(d) \sim d^{-\eta} \exp\left[- \left(\frac{d}{d_c} \right)^3 \right], \tag{2}$$

we found that in the stimulatory phase, the correlation scaling exponent is $\eta = 0.42$ and the characteristic correlation distance in pixels is $d_c = 102$ (Fig. 5 *A*). In the nonstimulatory phase, the scaling exponent is lower, $\eta = 0.33$, and the correlation distance is shorter, $d_c = 90$. A shorter correlation distance in the nonstimulatory phase reflects the fact that below the threshold glucose concentration, the collective response of β cells is still muted.

Because the cross-correlation function is an expectation of pair cross correlations, $C(d) = \langle C_{ij} \rangle = \mathbb{E}[C_{ij}]$, we could also calculate the associated variances, $\mathrm{Var}[C_{ij}]$. We found that the relationship between $\mathrm{Var}[C_{ij}]$ and $\mathbb{E}[C_{ij}]$ is linear, where two distinct lines corresponding to nonstimulatory and stimulatory phases have the same slope, $c_0 \approx 0.25$ (Fig. 5 *B*). This result provides additional insights into the nature of fast calcium oscillations. Intuitively, the cross correlation gets stronger if simultaneous spiking is more frequent. That $\mathrm{Var}[C_{ij}]$ and $\mathbb{E}[C_{ij}]$ are linearly related is a signature of a Poisson process, thus indicating that the number of simultaneous spikes in two signals recorded at a given distance is a Poission-distributed random variable. We further hypothesize that the number of simultaneous spikes is proportional to the number of gap junctions between nearby cells, in which case slope c_0 is interpretable as an elementary contribution of each cell-cell interaction to the cross correlation (53), whereas the estimated value of $c_0 \approx 0.25$ is in broad agreement with a previous report on collective chemosensing in micropatterned fibroblast cell colonies (53). The two distinct lines below and above the threshold glucose concentration are yet another sign that cell-to-cell communication within β-cell collectives qualitatively changes in response to glucose. The distinction between the two phases fades only at large distances at which cross correlations are very weak (*bottom left corner* in Fig. 5 *B*).

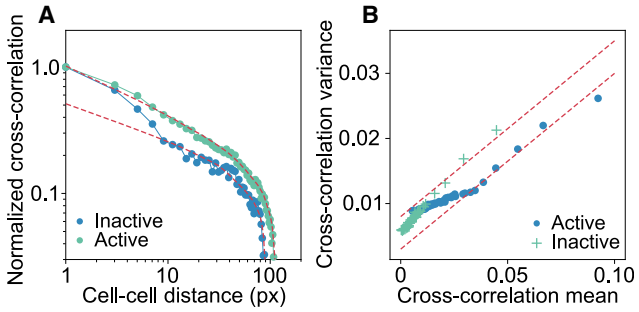

FIGURE 5 Cross-correlation of Ca^{2+} traces reflects a collective β-cell response to the threshold glucose concentration. (*A*) Shown is the ratio $C(d)/C(0)$ in nonstimulatory and stimulatory phases. For a large range of distances, the empirical cross correlation is interpretable as a combination of power law and faster-than-exponential decay but with different scaling exponents and correlation distances, mirroring in part a muted collective behavior in the nonstimulatory phase. (*B*) The linear relationship between the mean and the variance of empirical cross correlations is a signature of the Poisson process, yet the process differs below and above the threshold glucose concentration, as revealed by two distinct lines that fit the data. This linear relationship starts to break down for smaller cross-correlation means and thus larger distances at which faster-than-exponential cutoff kicks in (cf. *A*). To see this figure in color, go online.

DISCUSSION

This work attempts to understand the activity of insulin-secreting β cells as dynamical networks in which observed oscillatory phenomena emerge from cell-to-cell interactions within the spatial constraints of a typical islet rather than from the properties of single cells alone. On a spectrum of mathematical models mimicking β-cell function, our approach using simple coupled units (i.e., cells) sits at the opposite end of highly complex single units described with a system of differential-algebraic equations and subjected to deterministic coupling. In between, there are many possible model formulations that use more or less complex single unit dynamics or more or less stochastic couplings,

yet we steer clear of examining to what extent such more complex models account for the observations. We feel that it is important to emphasize this because our approach contains elements that some may find contentious (e.g., Hebbian-learning-like response to activity), although well-known models from the literature (45,54) may also be able to explain the distinct features of β-cell collectives (e.g., sensitivity to glucose stimulation that differs from the sensitivity of individual cells). In other words, our work should be seen as an attempt to offer a novel, to our knowledge, and simpler perspective on the documented phenomena, rather than invalidate previous work on which we, in fact, build.

In view of a rapid development of electrophysiological probes capable of detecting electrical (55,56) or optical (57) activities in pancreatic β cells, a further upgrade of our approach may eventually help to better understand physiology and pathophysiology of β-cell collectives and yield important cues for diagnosis, therapy, and prevention of diabetes mellitus (Remark 3 in the Supporting Materials and Methods). A way forward in this context would be to extract statistical properties of recorded signals, compare them with similar properties of simulated signals, and finally infer the model's parameter values for which recorded and simulated signals statistically best match each other. Inferred parameter values close to the critical point would then suggest a healthy β-cell function. Deviations from the critical point, by contrast, would serve as an early warning signal of a potentially degenerative condition (Fig. S7).

Particularly in relation to β-cell transplantation or better regeneration paradigms in type 1 diabetes mellitus, it is critical to understand to what extent β-cell collectives have to be replaced or regenerated to reestablish the healthy condition. Much more than just to transplant or regenerate an adequate β-cell mass, it is important to enable β-cell collectives to express dynamical cell-to-cell communication ability with a certain relative coupling strength. Our results could thus stimulate the development of novel diagnostic protocols to assess the improving function of β-cell collectives until full recovery. Although it is too early to decide on the merit of these specific ideas, the future does seem to be in the right intermix of affordable sensing technologies to acquire data, computational-statistical methods to analyze data, and—as much as complexity allows—mechanistic modeling to interpret data.

Data availability

Raw data analyzed in this study are made available through the Open Science Framework repository at http://doi.org/10.17605/OSF.IO/NA5H3.

SUPPORTING MATERIAL

Supporting Material can be found online at https://doi.org/10.1016/j.bpj.2020.04.005.

AUTHOR CONTRIBUTIONS

All authors contributed substantially to all aspects of the study.

ACKNOWLEDGMENTS

B.P. acknowledges financial support from the Slovenian Research Agency (project no. J5-8236), the University of Zagreb's project Advanced methods and technologies in Data Science and Cooperative Systems (ref. KK.01.1.1.01.009), and the University of Rijeka. D.K., M.S.K., A.S., J.D., and M.S.R. received financial support from the Slovenian Research Agency (research core funding program no. P3–0396 and projects no. N3-0048, no. N3-0133, and no. J3-9289). M.S.R. was further supported by the Austrian Science Fund/Fonds zur Förderung der Wissenschaftlichen Forschung (bilateral grants I3562–B27 and I4319-B). P.Ch.I. thanks the W. M. Keck Foundation, National Institutes of Health (grant 1R01-HL098437), Office of Naval Research (grant 000141010078), and US-Israel Binational Science Foundation (grant 2012219) for support. P.H. was supported by the Japan Society for the Promotion of Science Grant-in-Aid for Scientific Research (B) no. 18H01655 and the Grant for Basic Science Research Projects by the Sumitomo Foundation. Finally, M.J. was partially supported by the University of Rijeka. The funders had no role in study design, data collection and analysis, decision to publish, or preparation of the manuscript.

REFERENCES

1. Celiker, H., and J. Gore. 2013. Cellular cooperation: insights from microbes. *Trends Cell Biol.* 23:9–15.
2. Archetti, M., and K. J. Pienta. 2019. Cooperation among cancer cells: applying game theory to cancer. *Nat. Rev. Cancer.* 19:110–117.
3. Kim, A., K. Miller, …, M. Hara. 2009. Islet architecture: a comparative study. *Islets.* 1:129–136.
4. Dolenšek, J., M. S. Rupnik, and A. Stožer. 2015. Structural similarities and differences between the human and the mouse pancreas. *Islets.* 7:e1024405.
5. Korošak, D., and M. Slak Rupnik. 2018. Collective sensing of β-cells generates the metabolic code. *Front. Physiol.* 9:31.
6. Henderson, J. R. 1969. Why are the islets of Langerhans? *Lancet.* 2:469–470.
7. Cahill, G. F., Jr. 1971. The banting memorial lecture 1971. Physiology of insulin in man. *Diabetes.* 20:785–799.
8. Pipeleers, D., P. I. in't Veld, …, M. Van De Winkel. 1982. Glucose-induced insulin release depends on functional cooperation between islet cells. *Proc. Natl. Acad. Sci. USA.* 79:7322–7325.
9. Schwartz, M. W., R. J. Seeley, …, D. D'Alessio. 2013. Cooperation between brain and islet in glucose homeostasis and diabetes. *Nature.* 503:59–66.
10. Tokarz, V. L., P. E. MacDonald, and A. Klip. 2018. The cell biology of systemic insulin function. *J. Cell Biol.* 217:2273–2289.
11. Unger, R. H., and L. Orci. 2010. Paracrinology of islets and the paracrinopathy of diabetes. *Proc. Natl. Acad. Sci. USA.* 107:16009–16012.
12. Umpierrez, G., and M. Korytkowski. 2016. Diabetic emergencies - ketoacidosis, hyperglycaemic hyperosmolar state and hypoglycaemia. *Nat. Rev. Endocrinol.* 12:222–232.
13. MacDonald, P. E., J. W. Joseph, and P. Rorsman. 2005. Glucose-sensing mechanisms in pancreatic β-cells. *Philos. Trans. R. Soc. Lond. B Biol. Sci.* 360:2211–2225.
14. Skelin Klemen, M., J. Dolenšek, …, A. Stožer. 2017. The triggering pathway to insulin secretion: functional similarities and differences between the human and the mouse β cells and their translational relevance. *Islets.* 9:109–139.

15. Hellman, B. 1975. The significance of calcium for glucose stimulation of insulin release. *Endocrinology.* 97:392–398.
16. Prentki, M., and F. M. Matschinsky. 1987. Ca2+, cAMP, and phospholipid-derived messengers in coupling mechanisms of insulin secretion. *Physiol. Rev.* 67:1185–1248.
17. Henquin, J. C. 2011. The dual control of insulin secretion by glucose involves triggering and amplifying pathways in β-cells. *Diabetes Res. Clin. Pract.* 93 (*Suppl 1*):S27–S31.
18. Idevall-Hagren, O., and A. Tengholm. 2020. Metabolic regulation of calcium signaling in beta cells. *Semin. Cell Dev. Biol* Published online February 18, 2020. https://doi.org/10.1016/j.semcdb.2020.01.008.
19. Rorsman, P., L. Eliasson, …, S. Göpel. 2000. The cell physiology of biphasic insulin secretion. *News Physiol. Sci.* 15:72–77.
20. Rosario, L. M., I. Atwater, and E. Rojas. 1985. Membrane potential measurements in islets of Langerhans from ob/ob obese mice suggest an alteration in [Ca2+]i-activated K+ permeability. *Q. J. Exp. Physiol.* 70:137–150.
21. Valdeolmillos, M., R. M. Santos, …, L. M. Rosario. 1989. Glucose-induced oscillations of intracellular Ca2+ concentration resembling bursting electrical activity in single mouse islets of Langerhans. *FEBS Lett.* 259:19–23.
22. Caicedo, A. 2013. Paracrine and autocrine interactions in the human islet: more than meets the eye. *Semin. Cell Dev. Biol.* 24:11–21.
23. Capozzi, M. E., B. Svendsen, …, J. E. Campbell. 2019. β Cell tone is defined by proglucagon peptides through cAMP signaling. *JCI Insight.* 4:126742.
24. Jonkers, F. C., J. C. Jonas, …, J. C. Henquin. 1999. Influence of cell number on the characteristics and synchrony of Ca2+ oscillations in clusters of mouse pancreatic islet cells. *J. Physiol.* 520:839–849.
25. Rorsman, P., and G. Trube. 1986. Calcium and delayed potassium currents in mouse pancreatic beta-cells under voltage-clamp conditions. *J. Physiol.* 374:531–550.
26. Speier, S., A. Gjinovci, …, M. Rupnik. 2007. Cx36-mediated coupling reduces beta-cell heterogeneity, confines the stimulating glucose concentration range, and affects insulin release kinetics. *Diabetes.* 56:1078–1086.
27. Benninger, R. K., M. Zhang, …, D. W. Piston. 2008. Gap junction coupling and calcium waves in the pancreatic islet. *Biophys. J.* 95:5048–5061.
28. Head, W. S., M. L. Orseth, …, R. K. Benninger. 2012. Connexin-36 gap junctions regulate in vivo first- and second-phase insulin secretion dynamics and glucose tolerance in the conscious mouse. *Diabetes.* 61:1700–1707.
29. Chay, T. R., and J. Keizer. 1983. Minimal model for membrane oscillations in the pancreatic beta-cell. *Biophys. J.* 42:181–190.
30. Meyer-Hermann, M. E. 2007. The electrophysiology of the beta-cell based on single transmembrane protein characteristics. *Biophys. J.* 93:2952–2968.
31. Bertram, R., L. S. Satin, and A. S. Sherman. 2018. Closing in on the mechanisms of pulsatile insulin secretion. *Diabetes.* 67:351–359.
32. Stožer, A., R. Markovič, …, M. Gosak. 2019. Heterogeneity and delayed activation as hallmarks of self-organization and criticality in excitable tissue. *Front. Physiol.* 10:869.
33. Majdandzic, A., B. Podobnik, …, H. E. Stanley. 2014. Spontaneous recovery in dynamical networks. *Nat. Phys.* 10:34–38.
34. Podobnik, B., M. Jusup, …, H. E. Stanley. 2017. Biological conservation law as an emerging functionality in dynamical neuronal networks. *Proc. Natl. Acad. Sci. USA.* 114:11826–11831.
35. Speier, S., and M. Rupnik. 2003. A novel approach to in situ characterization of pancreatic beta-cells. *Pflugers Arch.* 446:553–558.
36. Stožer, A., J. Dolenšek, and M. S. Rupnik. 2013. Glucose-stimulated calcium dynamics in islets of Langerhans in acute mouse pancreas tissue slices. *PLoS One.* 8:e54638.
37. Bergsten, P. 1995. Slow and fast oscillations of cytoplasmic Ca2+ in pancreatic islets correspond to pulsatile insulin release. *Am. J. Physiol.* 268:E282–E287.
38. Gilon, P., R. M. Shepherd, and J. C. Henquin. 1993. Oscillations of secretion driven by oscillations of cytoplasmic Ca2+ as evidences in single pancreatic islets. *J. Biol. Chem.* 268:22265–22268.
39. Skelin, M., and M. Rupnik. 2011. cAMP increases the sensitivity of exocytosis to Ca^2+ primarily through protein kinase A in mouse pancreatic beta cells. *Cell Calcium.* 49:89–99.
40. Atwater, I., C. M. Dawson, …, E. Rojas. 1980. The nature of the oscillatory behaviour in electrical activity from pancreatic beta-cell. *Horm. Metab. Res. Suppl.* 10 (*Suppl 10*):100–107.
41. Stožer, A., J. Dolenšek, and M. S. Rupnik. 2013. Glucose-stimulated calcium dynamics in islets of Langerhans in acute mouse pancreas tissue slices. *PLoS One.* 8:e54638.
42. Colsoul, B., A. Schraenen, …, R. Vennekens. 2010. Loss of high-frequency glucose-induced Ca2+ oscillations in pancreatic islets correlates with impaired glucose tolerance in Trpm5-/- mice. *Proc. Natl. Acad. Sci. USA.* 107:5208–5213.
43. Barbero, A., and S. Sra. 2018. Modular proximal optimization for multidimensional total-variation regularization. *J. Mach. Learn. Res.* 19:2232–2313.
44. Loppini, A., A. Capolupo, …, G. Vitiello. 2014. On the coherent behavior of pancreatic beta-cell clusters. *Phys. Lett. A.* 378:3210–3217.
45. Smolen, P., J. Rinzel, and A. Sherman. 1993. Why pancreatic islets burst but single beta cells do not. The heterogeneity hypothesis. *Biophys. J.* 64:1668–1680.
46. Ravier, M. A., M. Güldenagel, …, P. Meda. 2005. Loss of connexin36 channels alters beta-cell coupling, islet synchronization of glucose-induced Ca2+ and insulin oscillations, and basal insulin release. *Diabetes.* 54:1798–1807.
47. Mantegna, R. N., and H. E. Stanley. 1995. Scaling behaviour in the dynamics of an economic index. *Nature.* 376:46–49.
48. Kiekens, R., P. In 't Veld, …, D. Pipeleers. 1992. Differences in glucose recognition by individual rat pancreatic B cells are associated with intercellular differences in glucose-induced biosynthetic activity. *J. Clin. Invest.* 89:117–125.
49. Benninger, R. K. P., and D. J. Hodson. 2018. New understanding of β-cell heterogeneity and in situ islet function. *Diabetes.* 67:537–547.
50. Damond, N., S. Engler, …, B. Bodenmiller. 2019. A map of human type 1 diabetes progression by imaging mass cytometry. *Cell Metab.* 29:755–768.e5.
51. Wang, Y. J., D. Traum, …, K. H. Kaestner; HPAP Consortium. 2019. Multiplexed in situ imaging mass cytometry analysis of the human endocrine pancreas and immune system in type 1 diabetes. *Cell Metab.* 29:769–783.e4.
52. Mears, D., N. F. Sheppard, Jr., …, E. Rojas. 1995. Magnitude and modulation of pancreatic beta-cell gap junction electrical conductance in situ. *J. Membr. Biol.* 146:163–176.
53. Sun, B., G. Duclos, and H. A. Stone. 2013. Network characteristics of collective chemosensing. *Phys. Rev. Lett.* 110:158103.
54. Hraha, T. H., M. J. Westacott, …, R. K. Benninger. 2014. Phase transitions in the multi-cellular regulatory behavior of pancreatic islet excitability. *PLoS Comput. Biol.* 10:e1003819.
55. Nguyen, Q. V., A. Caro, …, J. Lang. 2013. A novel bioelectronic glucose sensor to process distinct electrical activities of pancreatic beta-cells. *Conf. Proc. IEEE Eng. Med. Biol. Soc.* 2013:172–175.
56. Lebreton, F., A. Pirog, …, J. Lang. 2015. Slow potentials encode intercellular coupling and insulin demand in pancreatic beta cells. *Diabetologia.* 58:1291–1299.
57. Frank, J. A., J. Broichhagen, …, D. J. Hodson. 2018. Optical tools for understanding the complexity of β-cell signalling and insulin release. *Nat. Rev. Endocrinol.* 14:721–737.